Title

Co-Emergence of Specialized Endothelial Cells from Embryonic Stem Cells

Journal

Stem Cells and Development, 27(5)

ISSN

1547-3287

Authors

Madfis, Nicole
Lin, Zhiqiang
Kumar, Ashwath
et al.

Publication Date

2018-03-01

DOI

10.1089/scd.2017.0205

Peer reviewed

SCD-2017-0205-ver9-Madfis_1P
Type: research-article

STEM CELLS AND DEVELOPMENT
Volume 00, Number 00, 2018

DOI: 10.1089/scd.2017.0205

ORIGINAL RESEARCH REPORT

AU1 ▶

Co-Emergence of Specialized Endothelial Cells from Embryonic Stem Cells

AU2 ▶ Nicole Madfis,[1] Zhiqiang Lin,[2] Ashwath Kumar,[2] Simone A. Douglas,[3] Manu O. Platt,[3] Yuhong Fan,[2] and Kara E. McCloskey[1,4]

A well-formed and robust vasculature is critical to the health of most organ systems in the body. However, the endothelial cells (ECs) forming the vasculature can exhibit a number of distinct functional subphenotypes like arterial or venous ECs, as well as angiogenic tip and stalk ECs. In this study, we investigate the in vitro differentiation of EC subphenotypes from embryonic stem cells (ESCs). Using our staged induction methods and chemically defined mediums, highly angiogenic EC subpopulations, as well as less proliferative and less migratory EC subpopulations, are derived. Furthermore, the EC subphenotypes exhibit distinct surface markers, gene expression profiles, and positional affinities during sprouting. While both subpopulations contained greater than 80% VE-cad$^+$/CD31$^+$ cells, the tip/stalk-like EC contained predominantly Flt4$^+$/Dll4$^+$/CXCR4$^+$/Flt-1$^-$ cells, while the phalanx-like EC was composed of higher numbers of Flt-1$^+$ cells. These studies suggest that the tip-specific EC can be derived in vitro from stem cells as a distinct and relatively stable EC subphenotype without the benefit of its morphological positioning in the sprouting vessel.

Keywords: embryonic stem cells, endothelial cells, angiogenesis, tip cells, phalanx cells

Introduction

AU4 ▶ The field of vascular biology has firmly rejected the antiquated belief that blood vessels are merely ''plumbing'' for the distribution of blood. We now know that endothelial cells (ECs) play a dynamic role in regulating immune cell responses [1], leukocyte trafficking [2], vascular tone [3], blood coagulation and clotting [4], vascular permeability [5], tissue repair [6,7], and tumor growth [8]. In addition to the range of EC functions, EC specialization has been observed aligning with the specific needs of the tissue in which they reside [9–12] potentially designated before blood vessel maturation [13–15]. For example, arterial ECs are largely quiescent ECs that exhibit antithrombotic activity and release vasoactive molecules that control vessel relaxation. Conversely, postcapillary venular ECs are the primary site of trafficking for white blood cells [16,17]. EC morphology of the smallest arterioles is longer and narrower compared with arterial ECs. The microvascular ECs are involved in initiation of inflammatory signals following injury and infection, as well as angiogenesis and vascular pruning [16]. These ECs also exhibit distinct functions correlating with their anatomical location [13] and respond differentially to a variety of angiogenic stimuli [18,19]. The heterogeneity of EC genes expressed between tissue specific capillary beds reflects the importance of extracellular surface expression in function of EC subphenotypes [12].

Morphologically distinct vascular EC subphenotypes are also found within a sprouting blood vessel. Positioned at the leading edge of a sprouting vessel, ''tip'' ECs have been shown to upregulate delta-like ligand 4 (Dll4) [20,21], CXCR4 [22], Flt-4 [20,23], Nrp1 [20,24], and Unc5B [20], exhibit more organized stress fibers with numerous probing filopodia, and readily migrate toward an angiogenic stimulus [20]. However, tip ECs do not proliferate significantly or form lumens [20,25,26]. The ''stalk'' ECs are found trailing behind the tip ECs forming the stalk of the sprouting vessel. Unlike tip cells, stalk cells exhibit greater cell proliferation, lumen formation, increased extracellular matrix (ECM) production, and shorter filopodia [21]. Moreover, Notch signaling from the tip cells dampens the vascular endothelial growth factor (VEGF)-induced expression of Dll4 on stalk cells [20,21] allowing the tip cells to maintain their position at the leading edge of the sprouting vessel. It is thought that the downregulation of VEGFR2 (KDR/Flk-1) and Dll4 in the stalk cells also helps maintain balanced

[1]Graduate Program in Quantitative and System Biology, University of California, Merced, Merced, California.
[2]School of Biological Sciences and the Petit Institute for Bioengineering and Bioscience, Georgia Institute of Technology, Atlanta, Georgia.
AU3 ▶ [3]Wallace H. Coulter Department of Biomedical Engineering, Georgia Institute of Technology and Emory University.
[4]Department of Materials Science and Engineering, University of California, Merced, Merced, Georgia.

numbers of tip cells for more efficient sprouting and network formation [21].

There potentially exists a distinct nonsprouting, less proliferative, and less migratory EC subphenotype, named a ''phalanx'' EC [20,27]. These cells are recognized by their ''cobblestone'' morphology and high levels of soluble and membrane bound Flt-1 that mitigate VEGF signaling, as well as potentially increased extracellular VE-cadherin expression [20,27]. Although phalanx-type ECs are capable of responding to VEGF signaling, VEGF signaling in phalanx ECs acts as an apoptosis rescue from serum-deprived conditions, rather than as the migratory and proliferative responses seen in tip and stalk ECs [27]. The current dogma views the specification of an EC as a tip, stalk, or phalanx EC to be a stochastic process with ample plasticity and reversibility between these phenotypes during sprouting [25].

Using staged differentiation and chemically defined media to generate ECs from human and mouse ESCs [28–32], we discovered the co-emergence of sprouting tip and stalk-containing ECs and nonsprouting phalanx-containing ECs within our two-dimensional derivations [33]. Specifically, the phalanx ECs were purified from the tip/stalk-containing cultures, and both cultures sequentially expanded for up to 9–10 passages using the identical cell culture medium formulations. The expanded tip/stalk ECs stably exhibited increased levels of cell migration, proliferation, and increased vasculogenic- and angiogenic-like sprouting on Matrigel™ compared with the phalanx ECs [33]. The tip/stalk ECs also exhibited extensive and complex actin networks and phosphorylation of HSP27—required to release the cap ends from actin filaments and allow the generation of new polymerization required for cell migration [34,35]. Conversely, the phalanx-like ECs contained greater numbers of cells expressing Flt-1, Tie-1, and Tie-2 [33]. This was the first report of stable distinct subphenotypes emerging together in vitro from stem cells. Subsequently, a second group found that in vitro cultured sprouting ECs expressing low levels of CD143 exhibit enhanced angiogenic potential in alleviating local ischemia [36]. In this study, we further examined these distinct phenotypes for unique surface markers, gene expression profiles, gel degradation/remodeling, and positional affinities during sprouting. The results show that the tip-specific EC is a distinct and relatively stable EC subphenotype, even in the absence of its morphological association within the sprouting vessel.

Methods

Generation of tip/stalk-like and phalanx-like EC

The formulations and stage-specific derivation methodology (Fig. 1) using chemically defined mediums were conducted as previously reported [28,29,33]. Briefly, R1 murine embryonic stem cells (mESCs) were maintained on 0.5% gelatin coated plates in serum-free medium containing Knockout Dulbecco's modified Eagle's medium (KO-DMEM; Invitrogen), 15% Knockout Serum Replacer (KSR; Invitrogen), 1× Penicillin-Streptomycin (Invitrogen), 1× nonessential amino acids (Invitrogen), 2 mM L-glutamine (Invitrogen), 0.1 mM 2-mercaptoethanol (Calbiochem), 2,000 U/mL of leukemia inhibitory factor (LIF-ESGRO; Chemicon), and 10 ng/mL of bone morphogenetic protein-4 (BMP-4; R&D Systems). The initial induction that was induced using a medium optimized by our laboratory was named ''NS1D2b.'' This consists of alpha-MEM (Cellgro), 20% KSR (Invitrogen), 1 × penicillin-streptomycin (Invitrogen), 1 × nonessential amino acids (NEAA; Invitrogen), 2 mM L-glutamine (Invitrogen), 0.05 mM 2-mercaptoethanol (Calbiochem), 30 ng/mL of VEGF (R&D Systems), and 5 ng/mL BMP-4 (R&D Systems). After 2 days, the Flk-1^+ cells were stained with APC-conjugated anti-mouse CD309 (1:200, BioLegend) and viability fixative efluor760 (eBioscience) and enriched using Fluorescence Activated Cell Sorting (FACS, Aria II). The 10,000 Flk-1^+ cells/cm^2 were then seeded onto 50 μg/mL fibronectin-coated dishes in ''LDSk'' medium containing 70% alpha-MEM (Mediatech) and 30% DMEM (Invitrogen) plus 100 ng/mL VEGF (R&D Systems), 1% Nutridoma CS (Roche), 50 ng/mL bFGF (Sigma), 2 mM L-glutamine (Invitrogen), 1 × penicillin-streptomycin (Invitrogen), 1 × nonessential amino acids (Invitrogen), and 0.1 mM 2-mercaptoethanol (Calbiochem) [28]. After approximately 10 days, the cobblestone-shaped Flk-1^+ outgrowths were purified by manual selection (Fig. 1). These ECs have been shown to be consistent with phalanx EC subphenotype [33]. Both the selected phalanx-like and remaining nonselected tip/stalk-containing EC were subsequently maintained in a medium composed of 50% LDSk and 50% serum-free EGM-2™ supplemented with the EGM-2 BulletKit™ containing hydrocortisone, bFGF, VEGF, IGF, ascorbic acid, hEGF, heparin, and GA-1000 (Lonza), mixture called ''LDSF.''

Control EC

The isolation of primary mouse aortic endothelial cells (MAECs) from adult mice was approved by the Institutional Animal Care and Use Committee (IACUC) at the University of California, Merced. Briefly, adult 129/Sv+c/+p mice (Jackson Laboratories) were anesthetized using isoflurane before cervical dislocation. The abdominal aorta was excised, stripped of the tunica adventitia, cut into small pieces, and sandwiched on Matrigel drops with 0.1–0.2 mL of EBM-2 media (with EGM-2 BulletKit Supplements; Lonza) with 50 ng/mL VEGF. MAEC was allowed to migrate out of the aortas for 7 days before aortas were removed to prevent smooth muscle cell migration. MAEC outgrowths were purified using a combination of manual selection from the aorta outgrowths and then purified by FACS for CD31/CD144 positive cells. A commercially available immortalized murine cardiac endothelial cell (MCEC; CELLutions Biosystems) was also used, cultured in the same medium as described above.

Staining for FACS analysis

EC cultures were collected by incubating the cells with Cell Dissociation Buffer (Life Technologies) for 10 min and resuspended in PBS with 1% bovine serum albumin (BSA), mouse Fc Block (1:1,000; BD Biosciences), and fixable viability dye e780 (BD Biosciences). Live cells were stained for the following surface markers with corresponding IgG controls: anti-mouse CD31 PECy7 (1:200; BioLegend), anti-mouse Dll4 APC (1:400; BioLegend), anti-mouse Notch1 PE (1:200; eBioscience), anti-mouse VE-cad BV421 (1:400; BioLegend), anti-mouse Flt-4 Alexa Fluor® 488

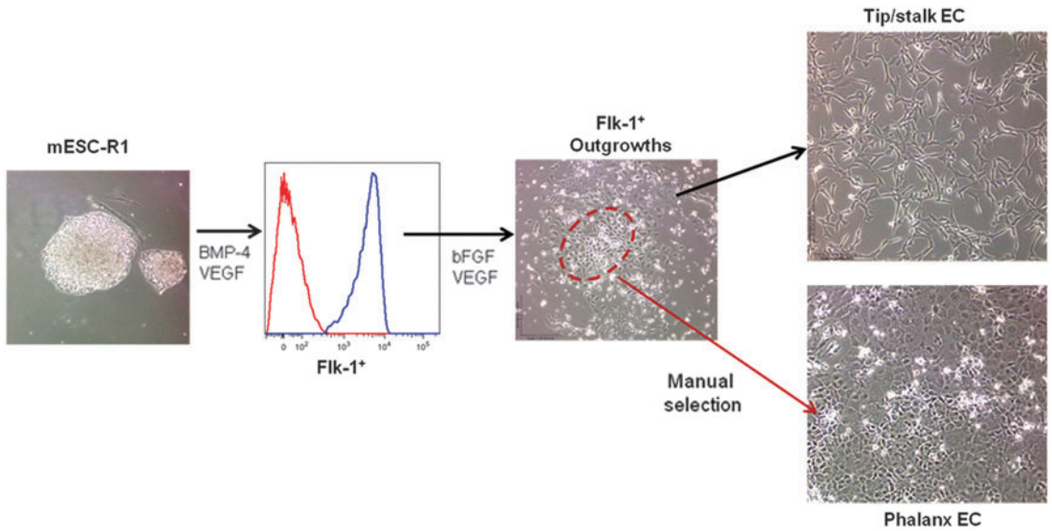

4C ▶ **FIG. 1.** Derivation of tip- and stalk-like EC and phalanx EC. Mouse ESCs were first induced into Flk-1$^+$ VPCs on fibronectin matrix in medium supplemented with BMP-4 and VEGF. The purified Flk-1$^+$ cells were then replated, again on fibronectin matrix in medium supplemented with bFGF and VEGF for EC specification. The Flk-1$^+$ outgrowths from the Flk-1$^+$ cells contained tip-, stalk-, and phalanx-like EC. These populations are then purified further with the cobblestone-shaped EC replated in a separate dish. These two EC subcultures maintain distinct subphenotypic expansion for ~10 passages. EC, endothelial cell; ESC, embryonic stem cell; VPC, vascular progenitor cell; VEGF, vascular endothelial growth factor.

(1:200; R&D), and anti-mouse Flt-1 Alexa Fluor 488 (1:100; RND systems). Titration optimizations were performed on all antibodies before analysis using fluorescence activated cell scanning (FACS; BD LSR II). Live cell populations were positively selected according to nonfluorescence and FSC/SSC dot plots. Data analysis and gating statistics were obtained using FlowJo software.

Staining for fluorescence imaging

Samples of purified cultures at passage 9 were fixed using 4% paraformaldehyde (PFA) for 15 min and permeabilized with 1% Triton (Sigma) for 5 min, then blocked in 5% donkey serum. Samples were incubated overnight in the following antibodies and compared against corresponding IgG controls: goat DDR2 (1:200; Santa Cruz), goat calponin-1 (1:200; Santa Cruz), and rabbit alpha-smooth muscle actin FITC (1:400; Santa Cruz). The secondary antibodies for anti-goat FITC (1:200; Santa Cruz) and anti-rabbit PE (1:200; Santa Cruz) were incubated for 1 h and counterstained with DAPI. Images were obtained using a Nikon Zeiss Microscope.

Fibrin bead sprouting assay

The tip/stalk-like EC was stained with 4 μm of CellTracker™ Green CMFDA Dye (Molecular Probes), while the phalanx-like EC was stained with 4 μm of CellTracker Red CMFDA Dye (Molecular Probes) for 45 min. EC cultures were filtered through a 70 μm nylon mesh filter and incubated with Cytodex® three microcarrier beads (200 cells per bead; Sigma) precoated with 50 μg/mL fibronectin. To facilitate attachment, the cell was placed on a nutator and incubated with microcarrier beads for 3 h. After confirming cell attachment, the cell-coated beads were resuspended in fresh media and incubated overnight. Fibrin gels were formed by resuspending cell-coated beads in 0.15 U/mL aprotinin and 2 mg/mL bovine plasma fibrinogen (Sigma). Bovine thrombin solution (0.625 U/mL; Sigma) was placed in the bottom of each well of a 24-well plate and the fibrinogen/bead-cell mixture was gently mixed into each well for 5 min, then allowed to polymerize at 37°C. After 15 min, 1 mL of ESC-EC maintenance media (LDSF) containing ~20,000 normal lung human fibroblasts (Lonza) was added to the top of each gel. The media was replaced every other day, and images were taken (Nikon Zeiss Microscope) every 24 h for up to 7 days (or until the fibrin gel degraded). Sprouting was quantified (sprout number and average length) on 100–150 beads per experimental condition.

RNA-Seq

Total RNAs were isolated with TRIzol reagent (Life Technologies) and RNAeasy Kit (Qiagen) according to the manufacturer's instructions. Ribo-Zero Gold rRNA Removal Kit (Illumina) was used to remove ribosomal RNA before preparation of sequencing libraries using the ScriptSeq RNA-Seq Library Prep Kit (Illumina). Sequencing was performed with Illumina HiSeq 4000 systems, and raw sequence reads were examined for quality using FastQC [37]. The reads were subsequently trimmed to remove adaptors and filtered for bad quality bases using Trim Galore [38,39]. Clean sequence reads were aligned to mouse genome, mm10, using STAR aligner [40]. Gene counts were called using HTSeq (5), and differentially expressed genes were identified using DESeq2 R package [41]. Gene ontology (GO) analysis was carried out using DAVID [42,43] to identify enriched biological functional groups and processes.

AU6 ▶ *Cathepsin and MMP zymography*

Total protein concentration was determined from the tip/stalk- and phalanx-containing EC lysates. Equal amounts were loaded for cathepsin or MMP zymography, as previously described [44,45]. Zymogram gels were imaged with an ImageQuant LAS 4000 (GE Healthcare), and densitometry was performed with ImageJ (NIH) to quantify cleared white bands, indicative of proteolytic activity.

Statistical analysis

Data are representative of at least three independent assays ($N=3$). Student's unpaired t-test was used to establish significance.

Results

Emerging tip/stalk and phalanx EC

To further delineate the subphenotype of co-emerging sprouting and nonsprouting EC subpopulations, we have F2 ▶ examined these subpopulations (Fig 2A), as well as two mouse EC control cell populations (Fig. 2B). In both EC subpopulations, EC markers Flk-1 [33], VE-cad, and CD31 were all expressed at high levels, with slightly greater expression of VE-cad and CD31 in the phalanx-like ECs compared to tip/stalk EC. Tip/stalk-containing EC subpopulations also consisted of higher numbers of tip-specific Dll4$^+$ [21] and Flt-4$^+$ [20,23] ECs and lower numbers of phalanx-specific Flt-1$^+$ cells [25,27] compared with phalanx-like EC. As one would expect, the EC marker expression profile of the emerging phalanx EC corresponded more closely with the MAEC and MCEC control cells compared with the tip/stalk-containing ECs (Fig. 2B). Extracellular expression of Nrp1 [20,24] and Jagged1 [46] was also analyzed, but not detected on any of the emerging EC subphenotypes or EC control cells (not shown).

Distinct EC subpopulations

To highlight the distinct subpopulations of EC, the tip/stalk and phalanx EC were co-stained for VE-cad, PECAM-1, Flt-1, and Dll4 (Fig. 2C). Both EC subpopulations contained 80%–90% PECAM-1$^+$/VE-cad$^+$ ECs, but a subset of the PECAM-1$^+$ (also called CD31$^+$) EC tip/stalk-containing cultures did not express VEGF decoy receptor, Flt-1, containing $\sim$20% Flt-1$^-$ cells, while the phalanx-containing cultures did not contain significant numbers of Flt-1$^-$ cells. These data corroborate that the Flt-1 marker is not expressed in the tip ECs [47].

Percentage of tip EC is a function of confluence

Because the percentage of Flt-1$^-$ ECs within tip/stalk-containing cultures varied significantly from derivation to derivation, it was hypothesized that the EC may be converting from Flt-1$^-$ tip-specific ECs to Flt-1$^+$ stalk-specific ECs as physical space for tip cell migration was mitigated with increasing confluence. Therefore, we compared tip/stalk EC cultured at lower confluence (50% dish coverage) with the same cells cultured at higher confluence (80% dish coverage). The tip/stalk ECs contained approximately 20% Flt-1$^-$ ECs when cultured at low confluence, but this number was reduced <5% in confluent cultures (Fig. 2D). These data suggest that either tip EC is not proliferating as robustly as the stalk EC or that the tip cells are converting to stalk cells as a result of greater numbers of cell-to-cell contacts in the confluent dishes.

EC subpopulations maintain phenotypic stability

The phenotypic stability of the emergent EC subpopulations was analyzed using a fibrin bead sprouting assay [48]. The tip/stalk-like EC (green) and phalanx-like EC (red) were coated onto dextran microcarrier beads independently and as a 1:1 mixture (Fig. 3). The tip/stalk-containing EC ◀F3 generated 2$\times$more sprouts per bead compared with the phalanx EC (Fig. 3A, B). The average sprout lengths for the tip/stalk EC were also 2$\times$longer compared with phalanx EC (Fig. 3C). When the tip/stalk (green) and phalanx (red) EC were mixed together, sprouting occurred more quickly (Fig. 3B) with total sprout numbers consistent with the tip/stalk EC. Moreover, the tip/stalk EC and phalanx EC self-organized within the angiogenic sprouts according to their preestablished subphenotypes—with the tip/stalk EC seen at the tips and stalks of the migrating sprouts and the phalanx EC located at the base of the sprout (Fig. 3A). Quantifying the contributing cells within these sprouts confirmed that 75% of the cells came from the tip/stalk EC subpopulation and only 25% from the phalanx EC (Fig. 3D).

Distinct gene expression patterns of EC subpopulations

To identify gene expression signatures associated with EC subpopulations, we performed RNA-Seq of the purified tip/stalk ECs and phalanx ECs, respectively. These two EC subpopulations display distinct expression profiles, and a total of 1,002 genes exhibit more than twofold expression changes (Fig. 4A). Compared to the tip/stalk-containing EC, ◀F4 670 genes were upregulated and 332 genes were downregulated in phalanx-containing EC (Fig. 4B). Gene ontology analysis suggested that different categories of gene signatures are associated with EC subpopulations. Compared with gene expression profiles in tip/stalk cells, the genes had higher expression in the phalanx-containing EC included in those known to be associated with mature EC function like wound healing, blood vessel morphogenesis, cell-to-cell adhesions, response to hypoxia, and regulation of cell proliferation. Other genes upregulated in phalanx EC include coagulation, thrombospondin, and lymphocyte trafficking selectin. The genes downregulated in the phalanx EC compared with the tip/stalk-containing EC encode regulation of proliferation, chromatin remodeling complexes, and histone proteins, suggesting that these cells are enriched in key biological processes regulating chromatin and cell proliferation.

Active matrix degrading proteases

To determine differences between the EC subphenotypes in active amounts of proteolytic enzymes capable of degrading ECM proteins and promoting angiogenesis, zymography was used on cell lysates from each of the cell populations. There were greater amounts of active MMP2 in the sprouting tip/stalk-containing EC compared with phalanx

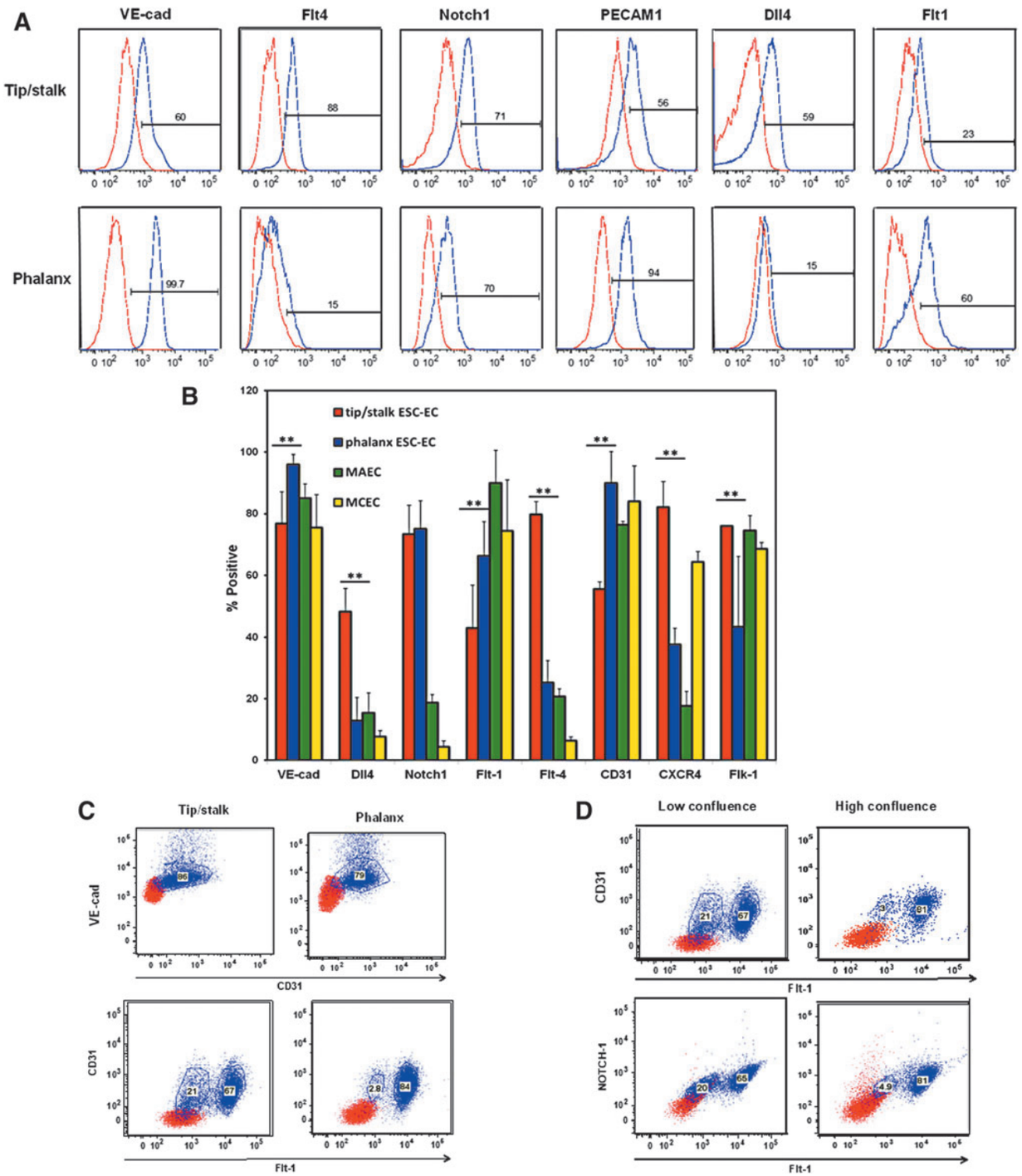

FIG. 2. Tip/stalk EC and phalanx EC differentially express specialized EC markers. **(A)** Representative single color histograms of tip/stalk-containing and phalanx-containing EC stained with a range of EC markers all plotted against isotype controls. **(B)** The mean percentages and standard deviations of tip/stalk-containing ($N=4$) and phalanx-containing EC ($N=4$), as well as mouse aortic endothelial cells (MAECs; $N=3$) to mouse cardiac endothelial cells (MCECs; $N=3$), control EC. Student's unpaired *t*-tests were used to establish significance between tip/stalk EC and phalanx EC, $^{**}P<0.001$. **(C)** Representative scatter plots of double stained tip/stalk-containing and phalanx-containing EC stained with VE-cad$^+$/CD31$^+$ and CD31$^+$/Flt-1$^+$ subsets. Note that mature EC markers VE-cad and CD31 indicate single EC population, but the Flt-1 marker indicates two distinct subpopulations in the tip- and stalk-containing EC. **(D)** Representative scatter plots of double stained tip/stalk-containing EC stained with CD31$^+$/Flt-1$^+$ and Notch1$^+$/Flt-1$^+$ subsets of tip/stalk EC cultured at low and high confluence show that the Flt-1$^-$ ECs are more prominent in cultures at low confluence. MAEC, mouse aortic endothelial cell.

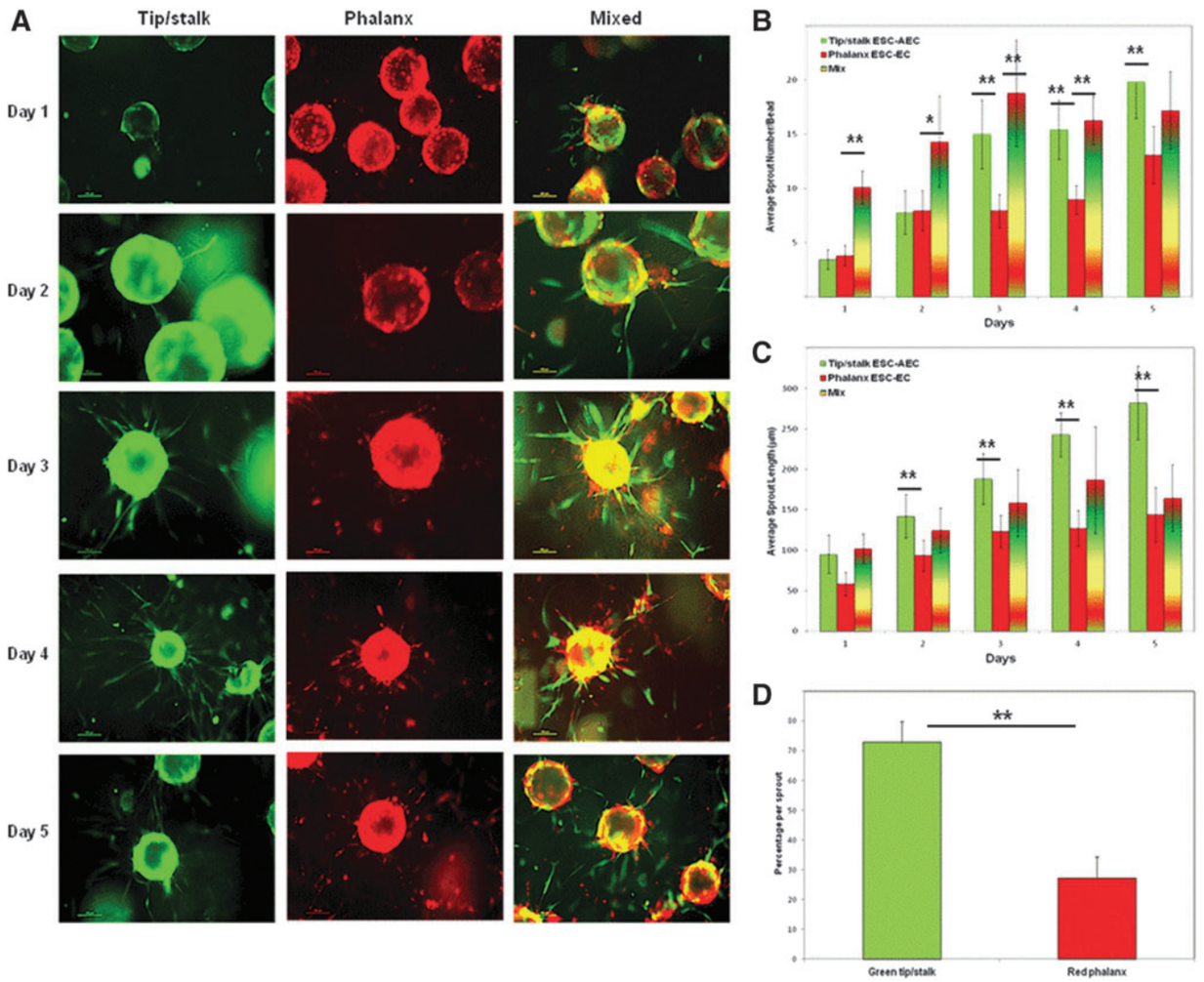

4C ▶

FIG. 3. Sprouting dynamics of tip/stalk- versus phalanx-containing EC. **(A)** Fluorescent images of sprouting tip/stalk EC (*green*) and phalanx EC (*red*) seeded separately and together on fibronectin-coated beads and embedded in fibrin gels, scale = 200 μm. **(B)** The average number of sprouts and **(C)** average sprout lengths were quantified for over 5 days. **(D)** The percentage of *green* and *red* cells in the sprouts of the mixed cells was also quantified on day 3. For each experimental condition, data were collected from 100 sprouting beads in three distinct assays ($N = 3$). Student's unpaired *t*-test was used to establish significance, $*P < 0.05$ and $**P < 0.001$.

F5 ▶

EC that contained greater levels of pro-MMP2, the zymogen form that must be cleaved to be active (Fig. 5A, B). Cathepsins are another class of proteases implicated in angiogenic pathways, and we profiled amounts of active cathepsins in the EC subphenotypes. Sprouting EC showed increased amounts of active cathepsins; specifically, greater cathepsin L activity was found in the sprouting tip/stalk-containing EC as indicated in the zymograms developed at pH 4, which is preferred for cathepsin L [45] (Fig. 5C, D). This was corroborated in the zymograms incubated at pH 6 by the 20 kDa band of active cathepsin L being significantly higher in the tip/stalk-containing EC, while the 15 and 22 kDa fragments were found in the phalanx EC (Fig. 5E, F). Taken together, ECM degrading enzymes appear to be involved in the sprouting behaviors of the tip/stalk EC, which may be associated with angiogenic pathways.

Discussion

Our results demonstrate the emergence of distinct sprouting and nonsprouting endothelial subphenotypes from Flk-1/KDR+ cells during in vitro EC-specific differentiation. Moreover, once sorted and cultured separately, these cells are phenotypically stable [33]. In addition to sprouting affinity, we identified that key distinctions between the sprouting cells and nonsprouting EC included expression of EC markers, gene expressions, and amounts of active cathepsins. Sprouting EC contained more cells expressing tip-specific $CXCR4^+$, $Dll4^+$, and $Flt\text{-}4^+$ markers and reduced numbers of $Flt\text{-}1^+$ cells. Co-staining for $CD31^+/Flt\text{-}1^+$ and $Notch\text{-}1^+/Flt\text{-}1^+$ verifies that two subpopulations of EC are present within the tip/stalk-containing EC, but not in the phalanx EC.

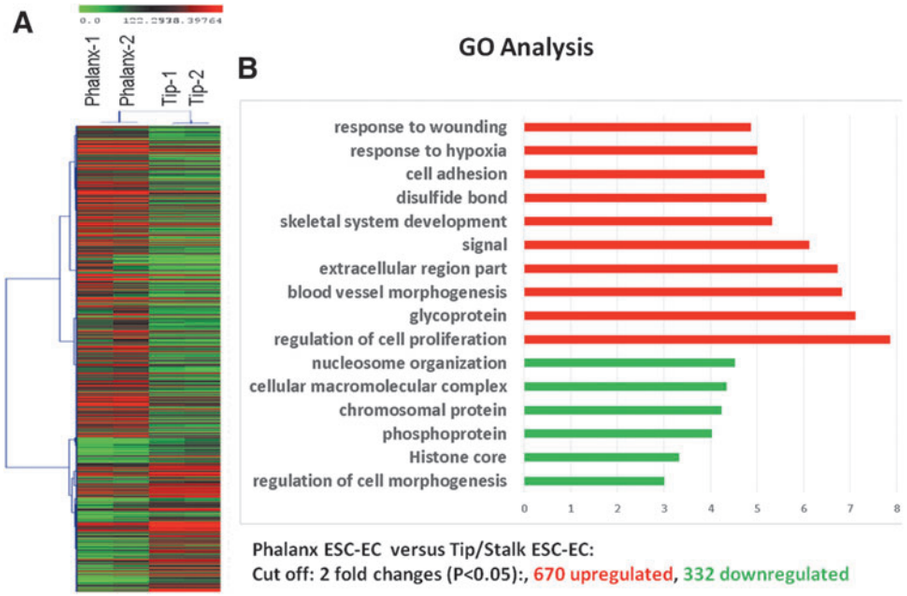

FIG. 4. Gene expression of phalanx-containing EC compared with tip/stalk-containing EC. **(A)** Hierarchical clustering analysis of genes upregulated (*red*) in phalanx EC compared with tip/stalk-containing EC, as well as genes downregulated (*green*) in phalanx EC compared with tip/stalk-containing EC. Genes with expression differences more than twofold were selected for analysis ($P < 0.05$). **(B)** GO Analysis of the differentially expressed genes. *x*-axis: -lg(*P* value). GO, gene ontology. ◀4C

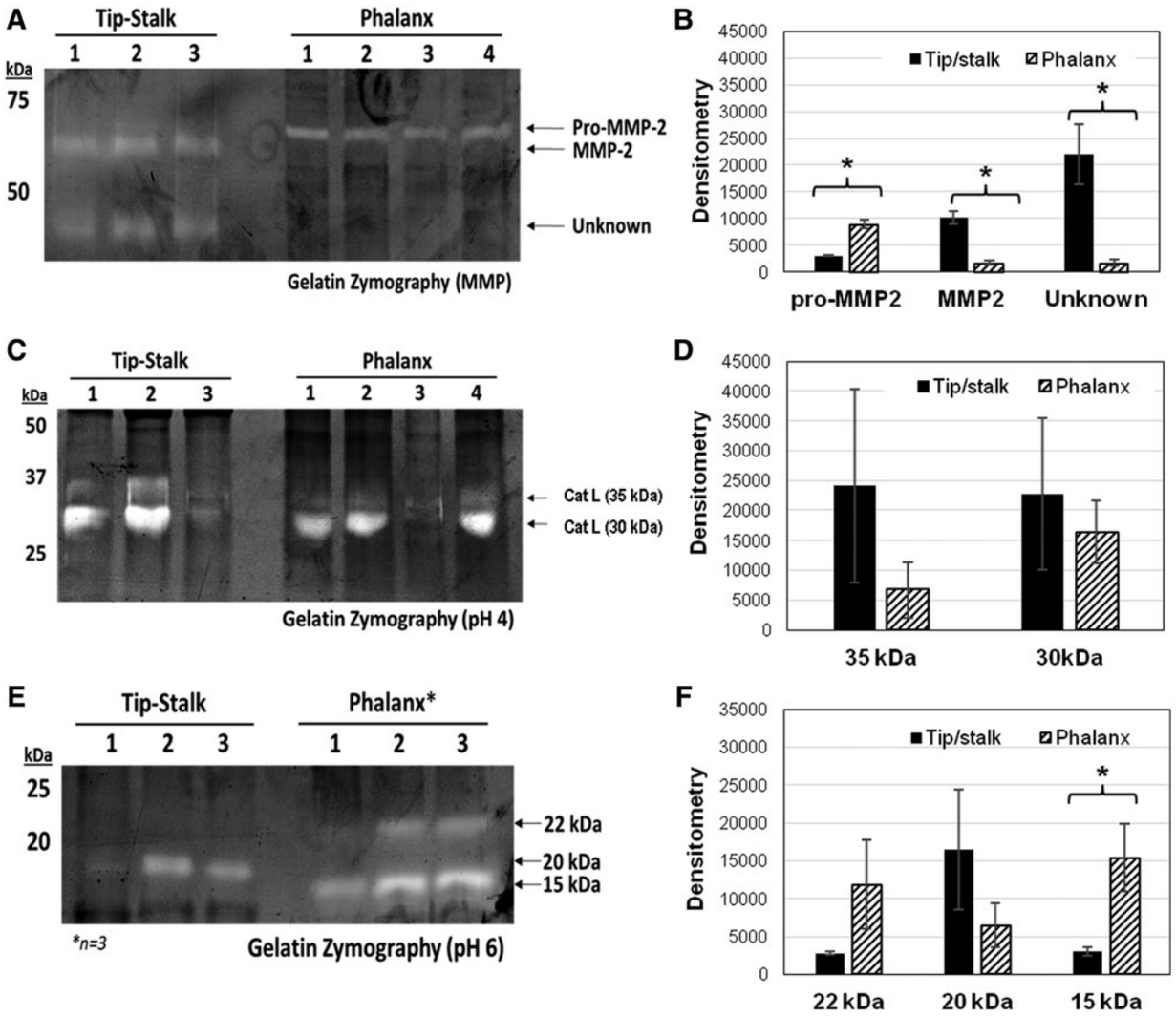

FIG. 5. Zymography Data. **(A, B)** Pro-MMP2 is greater in phalanx EC, while MMP2 is greater in tip/stalk-containing EC. **(C, D)** Cathepsin L expression at ph 4. **(E, F)** ph 6. *Indicates statistical significance at $P < 0.01$.

The stability of the tip/stalk-containing EC and phalanx EC subpopulations was also examined using a competitive sprouting assay. The tip/stalk-containing cells exhibited greater radial invasion compared with the phalanx EC, even if premixed and competing for morphological position. Most significantly, these findings provide convincing data challenging the previous thinking that sprouting ECs are homogeneous cells simply competing to maintain their morphological position within the sprouting vessel [49,50].

The appearance of sprouting tip EC in our vascular stem cell derivation cultures is relatively unique, only reported by one other group [36]. This observation is likely due to the following key elements: (a) the use of a staged derivation approach that purifies early Flk-1/KDR vascular and cardiovascular lineage-committed cells [28], (b) replacing fetal bovine serum (FBS), which is known to enhance the proliferation of contaminating smooth muscle cells [51], with a fully characterized serum-replacement (Nutridoma™-SP; Sigma-Aldrich), and (c) the incorporation of high levels of VEGF treatment known to strongly signal tip-specific EC within a sprouting blood vessel [26,52,53]. However, it is important to also note that the high levels of VEGF in the cell culture medium of the purified phalanx EC do not induce the phalanx-specific EC to revert to tip-specific ECs, providing more evidence that the tip cells are derived from vascular precursors and less likely derived from mature ECs. Note, while these studies suggest that the tip-specific EC is a distinct and relatively stable EC subphenotype from the phalanx EC, it remains unclear whether the phalanx EC is a distinct subphenotype, or if the phalanx EC is the same EC as a stalk EC in the absence of tip EC.

Thinking more deeply at what might be distinct in the tip/stalk-containing EC, we looked at the protease activity in the sprouting and nonsprouting cell populations and found—consistent with the invasive and migratory EC subphenotype of the tip/stalk-containing cells—increased matrix metalloprotease MMP2 activity and cathepsin L fragments in the sprouting EC subpopulations. Although increased cathepsin L is associated with cell invasion and neovascularization [54,55], it has been shown to be upregulated in endothelial progenitor cells compared with mature ECs [54,55]. However, its increased activity is not necessarily always associated with angiogenesis. In fact, Dennemarker et al., suggest a AU7 ► protective effect by mouse cathepsin L (CTSL) [56] whose substrates also include angiostatic peptides such as endostatin. At a slightly acidic pH, mouse Cathepsin L (catL) was higher in phalanx EC suggesting that catL is multifunctional and its context within specialized EC populations. The angiogenic shift that controls CTSL activity between EC subphenotypes is not clear. In humans, CTSL expression has been associated with an increase in angiogenic EC behaviors and increased expression in cell cycle genes that is consistent with highly increased proliferation necessary for vascular sprout elongation [57], but the mechanism has not yet been explored. It has been suggested that the invasive behaviors of the sprouting EC could be positively regulated through multiple pathways. ADAM17 leads to activation of MMP2 during angiogenesis [58], while overexpression of ADAM17 has been shown to reduce the expression of antiangiogenic molecules [59] and contribute to an invasive EC subphenotype [60].

Overall, this work shows that the sprouting and nonsprouting populations are differentially regulated as vascular endothelial subtypes. The nonsprouting cultures have increased expression of mature endothelial associated genes despite high $CD31^+$/VE-cad^+ populations in both cultures. The sprouting cultures have increased expression of chromatin remodeling complexes and associated genes, suggesting an important role of epigenetic control in EC subphenotype specification.

Conclusions

Currently, in vitro models of vascular biology almost exclusively use human umbilical vein endothelial cells. However, the use of human tip, stalk, or phalanx EC subphenotypes would more accurately reflect the EC biology being examined. Pro-angiogenic tip/stalk ECs would be most appropriate for studying angiogenesis and perhaps in microvascularization of tissue engineering products while the less proliferative and less migratory phalanx EC would be best for studies on atherosclerosis and perhaps better for lining small diameter vascular grafts [61,62]. The ability to derive and maintain distinct EC subphenotypes in vitro from mouse ESC, and eventually human ESC and iPS cells, is a significant advancement in the specification of differential EC fates and in developing appropriate in vitro models for studying angiogenesis, inflammation, vascular homeostasis, and disease.

Acknowledgments

This work was funded through a California Institute for Regenerative Medicine (CIRM) Basic Biology Award (#RB5-07414), as well as NSF-Science and Technology Center (STC) for the Emergent Behavior of Integrated Biological Systems (EBICS) Award # 0939511.

Author Disclosure Statement

The authors do not have any conflicts of interest with regard to this work.

References ◄AU8

1. Pober JS and WC Sessa. (2007). Evolving functions of endothelial cells in inflammation. Nat Rev Immunol 7:803–815.
2. Cines DB, ES Pollak, CA Buck, J Loscalzo, GA Zimmerman, RP McEver, JS Pober, TM Wick, BA Konkle, et al. (1998). Endothelial cells in physiology and in the pathophysiology of vascular disorders. Blood 91:3527–3561.
3. Furchgott RF and JV Zawadzki. (1980). The obligatory role of endothelial cells in the relaxation of arterial smooth muscle by acetylcholine. Nature 288:373–376.
4. Pearson JD. (1999). Endothelial cell function and thrombosis. Baillieres Best Pract Res Clin Haematol 12:329–341.
5. Michell BJ, JE Griffiths, KI Mitchelhill, I Rodriguez-Crespo, T Tiganis, S Bozinovski, PR de Montellano, BE Kemp and RB Pearson. (1999). The Akt kinase signals directly to endothelial nitric oxide synthase. Curr Biol 9: 845–848.
6. Butler JM, H Kobayashi and S Rafii. (2010). Instructive role of the vascular niche in promoting tumour growth and tissue repair by angiocrine factors. Nat Rev Cancer 10:138–146.

7. Baddour JA, K Sousounis and PA Tsonis. (2012). Organ repair and regeneration: an overview. Birth Defects Res C Embryo Today 96:1–29.
8. Rehman AO and CY Wang. (2006). Notch signaling in the regulation of tumor angiogenesis. Trends Cell Biol 16:293–300.
9. Aird WC. (2003). Endothelial cell heterogeneity. Crit Care Med 31:S221–S230.
10. Aird WC. (2006). Mechanisms of endothelial cell heterogeneity in health and disease. Circ Res 98:159–162.
11. Garlanda C, C Parravicini, M Sironi, M De Rossi, R Wainstok de Calmanovici, F Carozzi, F Bussolino, F Colotta, A Mantovani and A Vecchi. (1994). Progressive growth in immunodeficient mice and host cell recruitment by mouse endothelial cells transformed by polyoma middle-sized T antigen: implications for the pathogenesis of opportunistic vascular tumors. Proc Natl Acad Sci U S A 91:7291–7295.
12. Nolan DJ, M Ginsberg, E Israely, B Palikuqi, MG Poulos, D James, BS Ding, W Schachterle, Y Liu, et al. (2013). Molecular signatures of tissue-specific microvascular endothelial cell heterogeneity in organ maintenance and regeneration. Dev Cell 26:204–219.
13. Garlanda C and E Dejana. (1997). Heterogeneity of endothelial cells. Specific markers. Arterioscler Thromb Vasc Biol 17:1193–1202.
14. Lawson ND, N Scheer, VN Pham, CH Kim, AB Chitnis, JA Campos-Ortega and BM Weinstein. (2001). Notch signaling is required for arterial-venous differentiation during embryonic vascular development. Development 128:3675–3683.
15. Lawson ND, AM Vogel and BM Weinstein. (2002). sonic hedgehog and vascular endothelial growth factor act upstream of the Notch pathway during arterial endothelial differentiation. Dev Cell 3:127–136.
16. Chi JT, HY Chang, G Haraldsen, FL Jahnsen, OG Troyanskaya, DS Chang, Z Wang, SG Rockson, M van de Rijn, D Botstein and PO Brown. (2003). Endothelial cell diversity revealed by global expression profiling. Proc Natl Acad Sci U S A 100:10623–10628.
17. Eichmann A, L Yuan, D Moyon, F Lenoble, L Pardanaud and C Breant. (2005). Vascular development: from precursor cells to branched arterial and venous networks. Int J Dev Biol 49:259–267.
18. Lang I, C Hoffmann, H Olip, MA Pabst, T Hahn, G Dohr and G Desoye. (2001). Differential mitogenic responses of human macrovascular and microvascular endothelial cells to cytokines underline their phenotypic heterogeneity. Cell Prolif 34:143–155.
19. Brouillet S, P Hoffmann, M Benharouga, A Salomon, JP Schaal, JJ Feige and N Alfaidy. (2010). Molecular characterization of EG-VEGF-mediated angiogenesis: differential effects on microvascular and macrovascular endothelial cells. Mol Biol Cell 21:2832–2843.
20. De Smet F, I Segura, K De Bock, PJ Hohensinner and P Carmeliet. (2009). Mechanisms of vessel branching: filopodia on endothelial tip cells lead the way. Arterioscler Thromb Vasc Biol 29:639–649.
21. Hellström M, LK Phng, JJ Hofmann, E Wallgard, L Coultas, P Lindblom, J Alva, AK Nilsson, L Karlsson and N Gaiano. (2007). Dll4 signalling through Notch1 regulates formation of tip cells during angiogenesis. Nature 445:776–780.
22. Strasser GA, JS Kaminker and M Tessier-Lavigne. (2010). Microarray analysis of retinal endothelial tip cells identifies CXCR4 as a mediator of tip cell morphology and branching. Blood 115:5102.
23. Tammela T, G Zarkada, H Nurmi, L Jakobsson, K Heinolainen, D Tvorogov, W Zheng, CA Franco, A Murtomaki, et al. (2011). VEGFR-3 controls tip to stalk conversion at vessel fusion sites by reinforcing Notch signalling. Nat Cell Biol 13:1202–1213.
24. Gerhardt H, C Ruhrberg, A Abramsson, H Fujisawa, D Shima and C Betsholtz. (2004). Neuropilin 1 is required for endothelial tip cell guidance in the developing central nervous system. Dev Dyn 231:503–509.
25. Carmeliet P, F De Smet, S Loges and M Mazzone. (2009). Branching morphogenesis and antiangiogenesis candidates: tip cells lead the way. Nat Rev Clin Oncol 6:315–326.
26. Gerhardt H, M Golding, M Fruttiger, C Ruhrberg, A Lundkvist, A Abramsson, M Jeltsch, C Mitchell, K Alitalo, D Shima and C Betsholtz. (2003). VEGF guides angiogenic sprouting utilizing endothelial tip cell filopodia. J Cell Biol 161:1163–1177.
27. Mazzone M, D Dettori, R Leite de Oliveira, S Loges, T Schmidt, B Jonckx, YM Tian, AA Lanahan, P Pollard and C Ruiz de Almodovar. (2009). Heterozygous deficiency of PHD2 restores tumor oxygenation and inhibits metastasis via endothelial normalization. Cell 136:839–851.
28. Blancas A, Shih AJ, Lauer NE, McCloskey KE. (2011). Endothelial cells from embryonic stem cells in a chemically defined medium. Stem Cells Dev 20:2153–2161.
29. Blancas AA, NE Lauer and KE McCloskey. (2008). Endothelial differentiation of embryonic stem cells. Curr Protoc Stem Cell Biol Chapter 1:Unit 1F 5.
30. Glaser DE, RM Gower, NE Lauer, K Tam, AA Blancas, AJ Shih, SI Simon and KE McCloskey. (2011). Functional characterization of embryonic stem cell-derived endothelial cells. J Vasc Res 48:415–428.
31. McCloskey KE, I Lyons, RR Rao, SL Stice and RM Nerem. (2003). Purified and proliferating endothelial cells derived and expanded in vitro from embryonic stem cells. Endothelium 10:329–336.
32. McCloskey KE, SL Stice and RM Nerem. (2006). In vitro derivation and expansion of endothelial cells from embryonic stem cells. Methods Mol Biol 330:287–301.
33. Blancas AA, LE Wong, DE Glaser and KE McCloskey. (2013). Specialized tip/stalk-like and phalanx-like endothelial cells from embryonic stem cells. Stem Cells Dev 22:1398–1407.
34. Evans IM, G Britton and IC Zachary. (2008). Vascular endothelial growth factor induces heat shock protein (HSP) 27 serine 82 phosphorylation and endothelial tubulogenesis via protein kinase D and independent of p38 kinase. Cell Signal 20:1375–1384.
35. Piotrowicz RS, E Hickey and EG Levin. (1998). Heat shock protein 27 kDa expression and phosphorylation regulates endothelial cell migration. FASEB J 12:1481.
36. Silva EA, C Eseonu and DJ Mooney. (2014). Endothelial cells expressing low levels of CD143 (ACE) exhibit enhanced sprouting and potency in relieving tissue ischemia. Angiogenesis 17:617–630.
37. Andrews S. (2010). FastQC A Quality Control tool for High Throughput Sequence Data. www.bioinformatics.babraham.ac.uk/projects/fastqc/.
38. Krueger F. Trim Galore!: A wrapper tool around Cutadapt and FastQC to consistently apply quality and adapter trim-

ming to FastQ files., www.bioinformatics.babraham.ac.uk/projects/trim_galore/.
39. Martin M. (2011). Cutadapt removes adapter sequences from high-throughput sequencing reads. EMBnet. J 17:10–12.
40. Dobin A, CA Davis, F Schlesinger, J Drenkow, C Zaleski, S Jha, P Batut, M Chaisson and TR Gingeras. (2013). STAR: ultrafast universal RNA-seq aligner. Bioinformatics 29:15–21.
41. Love MI, W Huber and S Anders. (2014). Moderated estimation of fold change and dispersion for RNA-seq data with DESeq2. Genome Biol 15:550.
42. Huang da W, BT Sherman and RA Lempicki. (2009). Systematic and integrative analysis of large gene lists using DAVID bioinformatics resources. Nat Protoc 4:44–57.
43. Huang da W, BT Sherman and RA Lempicki. (2009). Bioinformatics enrichment tools: paths toward the comprehensive functional analysis of large gene lists. Nucleic Acids Res 37:1–13.
44. Li WA, ZT Barry, JD Cohen, CL Wilder, RJ Deeds, PM Keegan and MO Platt. (2010). Detection of femtomole quantities of mature cathepsin K with zymography. Anal Biochem 401:91–98.
45. Wilder CL, KY Park, PM Keegan and MO Platt. (2011). Manipulating substrate and pH in zymography protocols selectively distinguishes cathepsins K, L, S, and V activity in cells and tissues. Arch Biochem Biophys 516:52–57.
46. Moya IM, L Umans, E Maas, PN Pereira, K Beets, A Francis, W Sents, EJ Robertson, CL Mummery, D Huylebroeck and A Zwijsen. (2012). Stalk cell phenotype depends on integration of Notch and Smad1/5 signaling cascades. Dev Cell 22:501–514.
47. Krueger J, D Liu, K Scholz, A Zimmer, Y Shi, C Klein, A Siekmann, S Schulte-Merker, M Cudmore, A Ahmed and F le Noble. (2011). Flt1 acts as a negative regulator of tip cell formation and branching morphogenesis in the zebrafish embryo. Development 138:2111–2120.
48. Nakatsu MN, J Davis and CCW Hughes. (2007). Optimized fibrin gel bead assay for the study of angiogenesis. J Vis Exp 3:186.
49. Larrivee B, C Prahst, E Gordon, R del Toro, T Mathivet, A Duarte, M Simons and A Eichmann. (2012). ALK1 signaling inhibits angiogenesis by cooperating with the Notch pathway. Dev Cell 22:489–500.
50. Jakobsson L, CA Franco, K Bentley, RT Collins, B Ponsioen, IM Aspalter, I Rosewell, M Busse, G Thurston, et al. (2010). Endothelial cells dynamically compete for the tip cell position during angiogenic sprouting. Nat Cell Biol 12: 943–953.
51. Xie C, RP Ritchie, H Huang, J Zhang and YE Chen. (2011). Smooth muscle cell differentiation in vitro: models and underlying molecular mechanisms. Arterioscler Thromb Vasc Biol 31:1485–1494.
52. Cross MJ and L Claesson-Welsh. (2001). FGF and VEGF function in angiogenesis: signalling pathways, biological responses and therapeutic inhibition. Trends Pharmacol Sci 22:201–207.
53. Hirashima M, M Ogawa, S Nishikawa, K Matsumura, K Kawasaki and M Shibuya. (2003). A chemically defined culture of VEGFR2+ cells derived from embryonic stem cells reveals the role of VEGFR1 in tuning the threshold for VEGF in developing endothelial cells. Blood 101:2261–2267.
54. Reiser J, B Adair and T Reinheckel. (2010). Specialized roles for cysteine cathepsins in health and disease. J Clin Invest 120:3421–3431.
55. Urbich C, C Heeschen, A Aicher, K Sasaki, T Bruhl, MR Farhadi, P Vajkoczy, WK Hofmann, C Peters, et al. (2005). Cathepsin L is required for endothelial progenitor cell-induced neovascularization. Nat Med 11:206–213.
56. Dennemarker J, T Lohmuller, J Mayerle, M Tacke, MM Lerch, LM Coussens, C Peters and T Reinheckel. (2010). Deficiency for the cysteine protease cathepsin L promotes tumor progression in mouse epidermis. Oncogene 29:1611–1621.
57. Sudhan DR, MB Rabaglino, CE Wood and DW Siemann. (2016). Cathepsin L in tumor angiogenesis and its therapeutic intervention by the small molecule inhibitor KGP94. Clin Exp Metastasis 33:461–473.
58. Gooz P, M Gooz, A Baldys and S Hoffman. (2009). ADAM-17 regulates endothelial cell morphology, proliferation, and in vitro angiogenesis. Biochem Biophys Res Commun 380:33–38.
59. Caolo V, G Swennen, A Chalaris, A Wagenaar, S Verbruggen, S Rose-John, DG Molin, M Vooijs and MJ Post. (2015). ADAM10 and ADAM17 have opposite roles during sprouting angiogenesis. Angiogenesis 18:13–22.
60. Weskamp G, K Mendelson, S Swendeman, S Le Gall, Y Ma, S Lyman, A Hinoki, S Eguchi, V Guaiquil, K Horiuchi and CP Blobel. (2010). Pathological neovascularization is reduced by inactivation of ADAM17 in endothelial cells but not in pericytes. Circ Res 106:932–940.
61. Teebken OE and A Haverich. (2002). Tissue engineering of small diameter vascular grafts. Eur J Vasc Endovasc Surg 23:475–485.
62. Borschel GH, YC Huang, S Calve, EM Arruda, JB Lynch, DE Dow, WM Kuzon, RG Dennis and DL Brown. (2005). Tissue engineering of recellularized small-diameter vascular grafts. Tissue Eng 11:778–786.

Address correspondence to: ◀AU9
Kara E. McCloskey, PhD
School of Engineering
University of California, Merced
5200 N. Lake Road
Merced, CA 95343

E-mail: kmccloskey@ucmerced.edu

Received for publication January 9, 2018
Accepted after revision January 9, 2018
Prepublished on Liebert Instant Online XXXX XX, XXXX

AUTHOR QUERY FOR SCD-2017-0205-VER9-MADFIS_1P

AU1: Please note that gene symbols in any article should be formatted as per the gene nomenclature. Thus, please make sure that gene symbols, if any in this article, are italicized.
AU2: Please review all authors' surnames for accurate indexing citations.
AU3: Please mention the city and country name in affiliation 3.
AU4: The Publisher requests for readability that no paragraph exceeds 15 typeset lines. Please check for long paragraphs and divide where needed.
AU5: The acronym ''MCEC'' has been defined as ''murine cardiac endothelial cell'' and ''mouse cardiac endothelial cell.'' Please fix both for consistency.
AU6: Please define ''MMP'' if necessary.
AU7: Please confirm the expansions of ''CTSL'' and ''catL'' as both are defined as ''mouse cathepsin L.''
AU8: Ref. 49 has been deleted as it was a duplicate of Ref. 33, and Ref. citations in the text have been renumbered accordingly. Please check.
AU9: The address of the corresponding author mismatches with the given affiliation. Please check.
AU10: Figures 2 and 3 are poor quality. Please provide better quality figure.